



Seismic performance of RC bridge piers reinforced with high-strength steel bars: experimental study and numerical simulation

J.S. Su⁽¹⁾, D.Q. Wu⁽²⁾, Y. Ding⁽³⁾, Z.X. Li⁽⁴⁾

⁽¹⁾ Lecturer, Key Laboratory of Coast Civil Structure Safety of Ministry of Education, Tianjin University, China, junshengsu@tju.edu.cn

⁽²⁾ Ph.D Candidate, College of Civil Engineering, Tianjin University, China, aboutwdq@163.com

⁽³⁾ Professor, Key Laboratory of Coast Civil Structure Safety of Ministry of Education, Tianjin University, China, dingyang@tju.edu.cn

⁽⁴⁾ Professor, Key Laboratory of Coast Civil Structure Safety of Ministry of Education, Tianjin University, China, zxli@tju.edu.cn

Abstract

In order to promote the application of high-strength steel bars (HSSB) in RC bridge structures, the seismic performance of reinforced concrete (RC) bridge piers were studied by experimental study and numerical simulation. First, monotonic loading and low cycle fatigue tests of conventional steel bars (CSB) HRB400 and high-strength steel bars (HSSB) HTRB600 with different slenderness ratios (L/D) were conducted to investigate the mechanical properties of HSSB. The material tests indicate that the increase in yield strength and slenderness ratio would intensify the pinching effect of reinforcing steel material under compression, and reduce the low-cycle fatigue life of steel bars. Then, cyclic loading tests of ten rectangular RC bridge piers reinforced with different grades of longitudinal bar (i.e., HRB400E and HTRB600) were conducted to study the seismic performance of RC piers with different steel grades, stirrup layouts, concrete strengths and axial load ratios. The experimental results showed that all RC piers presented typical flexural failure mode that buckling and followed by low-cycle fatigue fracture of longitudinal bar. The increase in yield strength of longitudinal steel bars would reduce the post-cracking stiffness and then the hysteretic dissipated energy of RC piers. The RC piers reinforced with HSSB as longitudinal bars show comparable deformation capacity. When using higher strength concrete, the RC piers have smaller yield displacement and relatively lower deformation capacity, and the influence extent is more distinct with the increase of concrete strength. By comparisons between different configuration details of transverse reinforcement, the RC piers with two cross-ties within closed-hoop (type III) showed better ductility than that with one cross-ties (type I and type II) when using identical stirrup ratio, because this configuration provided better constraints to prevent buckling of longitudinal bars. The effect extent is more remarkable for RC piers with high axial load ratio. Thus, special attention should be paid to prevent buckling and low-cycle fatigue damage of high-strength steel bars in seismic design of RC piers to ensure deformation demand. Finally, a fiber-based nonlinear beam column element considering bar buckling, low-cycle fatigue and bond slip (strain penetration) was used to simulate the nonlinear response of RC piers, wherein the material parameters were calibrated according to the mechanical tests of CSB and HSSB. The hysteretic performance (maximum lateral loading, deformation capacity and total hysteretic dissipated energy) of RC piers were used to verify the reliability of finite element method (FEM). The results show that the FEM used in this paper could predict the nonlinear response and damage development progress of RC piers reinforced with varying yield strength steel bars.

Keywords: RC bridge piers, seismic performance, high-strength steel bars (HSSB), low-cycle fatigue, bar buckling



1. Introduction

The use of high-strength steel bars (HSSB) in reinforced concrete (RC) elements offers many advantages, such as reducing steel congestion and enhancing bearing capacity, as well as reducing costs associated with the transport and placement of steel material. Thus, RC design codes in many countries have lately become more receptive of the idea of using higher yield strength reinforcement in RC members, as introduced in Ref.[1].

Studies on the use of HSSB in concrete structures have been ongoing for some time. Among these researches, seismic performance of concrete structures reinforced with HSSB has attracted increasing attention from researchers and engineers. Particular interest has been around the concern that use of HSSB may result in inadequate ductility of the members because of larger yield stress and smaller fracture strain of high strength reinforcing steel material.

To make recommendations to the utilization of HSSB in concrete structures subjected to earthquake, Rautenberg et al [2][3], Cheng et al [4], Tavallali et al [5] and Barbosa et al [6][7] compared seismic performance of RC members using CSB Grade 60 (420MPa) and reduced amount of HSSB Grade 80 (550MPa), Grade100 (690MPa), Grade120 (827MPa) as well as SD685 (685MPa). These work indicated that replacing CSB Grade60 (420MPa) by proportionally reduced amounts of HSSB (to the increase in f_y), the RC columns presented comparable flexural strength and deformation capacity, but lower hysteretic dissipated energy.

Investigation following the 2016 Kaikoura earthquake [8] revealed a large number of bridge piers suffering bar buckling failure at the pier bottom. Bar buckling has significant effect on constitutive model of reinforcing steel [9]-[11], which then affects the seismic response of RC members, especially at the later stage of inelastic cyclic loading [12]-[15]. Fracture of longitudinal steel bars due to low-cycle fatigue is one of the prominent failure modes of RC bridge piers under strong earthquake motions, which induce large cyclic strain amplitude of the reinforcing steel at the pier bottom.

Dhakal and Maekawa [16] pointed out based on finite element analysis (FEA) that the post-buckling strain softening was more serious for higher strength reinforcing steel. Ghannou and Slavin [17] compared the low-cycle fatigue behavior of HSSB Grade 80 (550 MPa) with CSB Grade 60 (420 MPa), and indicated that significant difference existed between the fatigue life of HSSB and CSB. Besides, experimental studies have shown that bar buckling has detrimental effect on low-cycle fatigue life of reinforcing steel, and the increase in slenderness ratio (L/D) would result in substantial reduction to the low-cycle fatigue life [18][19]. Therefore, it is necessary to study the buckling and low-cycle fatigue properties of HSSB in order to better study the seismic performance of RC piers reinforced with HSSB.

The HSSB with yield strength of 600 MPa had been introduced to the latest chinese reinforcing steel code GB1499.2-2018 [20] (equivalent to an ASTM specification), however it has not been adopted in concrete structure codes [21] or bridge design code [22]. The main reasons for the limits on the use of HSSB are the lack of experimental data on RC piers (columns) constructed with HSSB, and the past experiences that increasing the yield strength of steel bars usually leads to a decrease in material strain ductility. Especially for the 600MPa HSSB used in China, only few experimental research [1][23][24] were conducted on the seismic behavior of RC members, which could not provide enough validation to utilize the HSSB. Therefore, the objective of this investigation is to explore the potential of using HSSB as flexural steel reinforcement in RC bridge piers in seismic regions through systematic experiments and numerical simulation .

2. Experimental program

Ten rectangular large scale RC bridge piers were tested under cyclic lateral loading and simultaneously constant axial load. The aspect ratio (L/D) of the tested specimens was 4.0. The applied axial load ratios were 0.1 and 0.3. The effects of the yield strength of longitudinal steel bars (i.e. HRB400E and HTRB600) on seismic performance of RC bridge piers were investigated with two steel replacement methods (i.e. equivalent strength and equivalent volume replacements). Besides, different transverse reinforcement layouts were adopted to study the effects of stirrup configurations on seismic performance of RC piers.



2.1 Specimen detailing

Figure 1 shows the details and configurations of the steel reinforcement in tested specimens. As can be seen in Table 1, the tested specimens consisted of ten rectangular RC piers with 520×400 mm section dimension, and the height of all piers was 2.0 m. The tested series were designed to investigate the effects of the yield strengths of longitudinal bar, concrete compressive strengths, axial load ratios and transverse reinforcement configurations on the seismic performance of RC piers. To identify the steel bars used in different specimens, L and H were used to represent the type of steel bars used herein, where L and H respectively represent HRB400 (low) and HTRB600 (high) steel bars. Two different steel replacement methods, equivalent volume and equivalent strength replacement, were adopted herein. For equivalent volume replacement, identical steel configuration and equal steel amount were used while only the yield strengths of steel bars were varied, and the label (V) was used to represent the series. As for equivalent strength replacement, the yield strength of steel bars times reinforcement ratio was kept constant, which can be expressed as $\rho_s f_{y1} = \rho_s f_{y2}$. C40, C60 and C80 are used to represent different strengths of concrete material. The axial load ratios 0.1 and 0.3 were adopted to study the effects of axial load ratios. Type I, II and III means different types of transverse reinforcement configurations, as shown in Figure 1. In order better observe the bar buckling at the pier bottom, the cover concrete outside the longitudinal bars at plastic hinge regions for most of RC piers was removed when producing the piers while the contrast specimens reserved the cover concrete which is identified using C at the end of the label.

Table 1 – Details of all test specimens

Specimen	Longitudinal Steel					Transverse Steel				Concrete		Axial load ratio
	d_b (mm)	Class	N o.	ρ_l (%)	d_s (mm)	Class	s (mm)	ρ_s (%)	Type	Class	Cover (mm)	
LC40-0.1-I	20	HRB400	16	2.40	8	HTRB600	60	0.99	I	C40	0	0.1
HC40-0.1-I	16	HTRB600	16	1.55	8	HTRB600	60	0.99	I	C40	0	0.1
H(V)C40-0.1-I	20	HTRB600	16	2.42	8	HTRB600	60	0.99	I	C40	0	0.1
HC40-0.1-I-C	16	HTRB600	16	1.55	8	HTRB600	60	0.99	I	C40	25	0.1
HC60-0.1-I-C	16	HTRB600	16	1.55	8	HTRB600	60	0.99	I	C60	25	0.1
HC80-0.1-I	16	HTRB600	16	1.55	8	HTRB600	60	0.99	I	C80	0	0.1
HC40-0.3-I	16	HTRB600	16	1.55	8	HTRB600	60	0.99	I	C40	0	0.3
HC40-0.1-II	16	HTRB600	16	1.55	8	HTRB600	65	1.05	II	C40	0	0.1
HC40-0.1-III	16	HTRB600	16	1.55	8	HTRB600	75	1.06	III	C40	0	0.1
HC40-0.3-III	16	HTRB600	16	1.55	8	HTRB600	75	1.06	III	C40	0	0.3

2.2 Material properties

Tensile tests of three random steel bar samples for each type of steel material were conducted in accordance to the GB/T 228.1-2010 [25]. The mechanical properties of steel bars are taken as the average value of three test results, as shown in Table 2. In the Table, ϵ_{rup} and ϵ respectively represent the fracture elongation and the ultimate uniform elongation. f_y and f_u are the yield stress and ultimate stress. It is shown in Figure 2(b) that the high-strength flexural steel reinforcement HTRB600 exist distinct yield plateau. Table 2 shows that tensile-to-yield strength ratio (T/Y) is greater than or equal to 1.25, the measured yield strength to defined yield strength ratio (f_y/f_{yk}) is smaller than or equal to 1.25, and the ultimate uniform elongation (ϵ) is bigger than 9%. In addition, to study the buckling and low-cycle fatigue characteristics of reinforcing steel, the low-cycle fatigue tests of steel materials with varying slenderness ratio (L/D) were conducted. The low-cycle fatigue test results will be shown in the following section.

Table 2 – Mechanical properties of reinforcing steel bars

Type	Class	d_b (mm)	f_{yk} (MPa)	f_y (MPa)	f_u (MPa)	E_s (MPa)	f_y/f_{yk}	f_u/f_y	ϵ_{rup} (%)	ϵ (%)
Longitudinal	HRB400E	20	400	454	606	2.27×10^5	1.14	1.33	34.5	13.1
	HTRB600	16	600	609	786	1.97×10^5	1.02	1.26	25.2	11.7
Transverse	HTRB600	20	600	625	816	2.03×10^5	1.04	1.31	25.3	12.3
		8	600	623	926	2.02×10^5	1.04	1.49	25.3	10.3

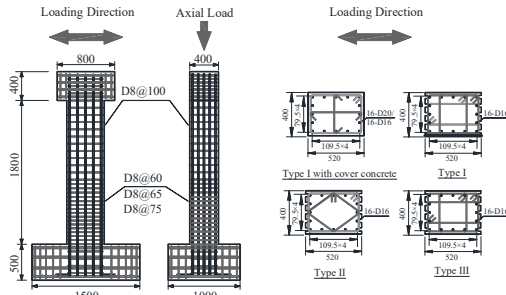


Fig. 1 – Geometry and reinforcement details of tested specimens

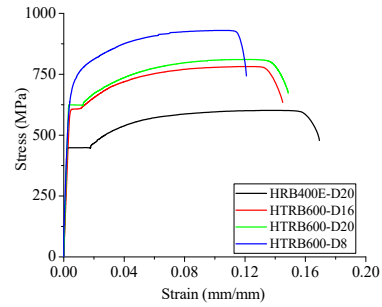


Fig. 2 – mechanical properties of the reinforcing steel

The mechanical properties of concrete material were obtained according to GB/T50152 [26]. Six standard cube specimens (150×150×150mm) were poured and maintained with the same condition as the RC bridge pier specimens. The measured cube compressive strengths f_{cu} respectively were 42.5 MPa, 59.6 MPa, and 81.7 MPa. While the corresponding axial compressive strength f_c and elastic modulus E_c are calculated according to GB/T50152 [26]. All concrete material mechanical parameters are shown in Table 3.

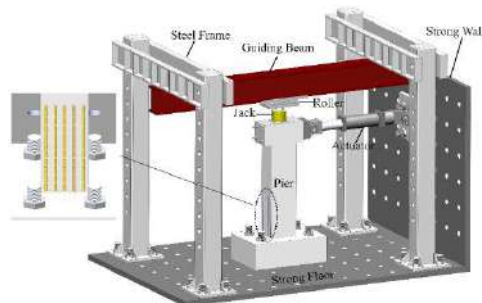
Table 3 – Mechanical properties of concrete material

Class	f_{cu} (MPa)	f_c (MPa)	E_c (MPa)	f_t (MPa)
C40	42.5	32.3	3.32×10^4	3.11
C60	59.6	46.5	3.59×10^4	3.74
C80	81.7	67.0	3.81×10^4	3.99

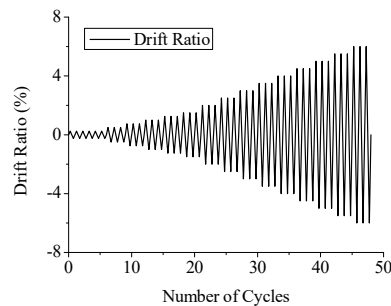
2.3 Loading procedure

The specimens were tested under the constant axial loading and cycle lateral loading, as shown in Fig. 3. The setup was initiated with stressing the pier footing to the strong floor through ground anchorage (Fig. 3(a)). The axial load was applied to the top of the specimens through a hydraulic jack that was located between the pier top and steel guiding beam. The lateral load was applied by a displacement-controlled hydraulic actuator with a capacity of 1000 kN, which was supported against the strong wall. The axial load was first applied to the target value and a pair of rollers were used to allow for slipping and rotation of the hydraulic jack.

A prescribed quasi-static cyclic loading scheme (as shown in Figure 3(a)) was laterally imposed to the top of the RC piers by displacement-controlled hydraulic actuator. The displacement increase amplitude was 5mm before 30mm and 10 mm after that. For each target displacement, three repeated displacement cycles were applied to capture the strength degradation, as shown in Fig.3 (b). The test was terminated when fracture of longitudinal steel bars was observed.



(a) Schematic loading diagram of RC bridge piers



(b) Loading diagram

Fig. 3 – Loading diagram of RC bridge piers

3. Experimental results

3.1 Reinforcing steel



In order to better study the seismic performance of RC piers, the buckling and low-cycle fatigue properties of reinforcing steel are studied. To compare the buckling properties of different yield strengths of steel bars, the normalized compressive stress-strain curves of reinforcing steel with different slenderness ratios (L/D) are compared, as shown in Fig.4. We can see from Fig.4 that the strain softening of steel material intensifies with the increase of slenderness ratio (L/D) under compression loading. Besides, the post-buckling strain softening is more serious for HSSB HTRB600 than that of CSB HRB400E, as pointed out in reference [16].

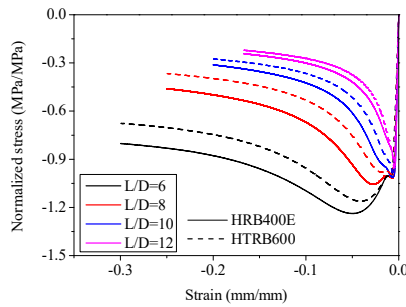


Fig. 4 – Normalized compressive stress-strain curves of reinforcing steel

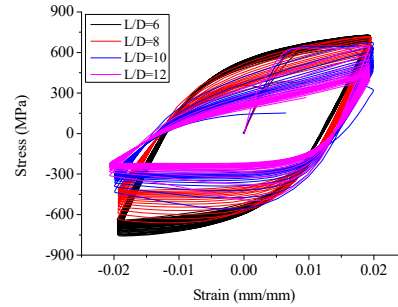


Fig. 5 –Cyclic curves of reinforcing steel with different slenderness ratios

The low-cycle fatigue tests of reinforcing steel material with 20mm diameter and varying slenderness ratios (i.e. $L/D=6,8,10,12$) were conducted. The strain amplitudes (unidirectional) used in the tests includes 1%, 1.5%, 2.0%, 3%, 4% and 5%. Coffin and Manson[27][28] firstly proposed an equations relating strain amplitude to the numbers of cycle to failure, as shown in Eq.(1). Where ε_p is the plastic strain amplitude (maximum value minus minimum value), C_f is a material constant to be determined from fatigue testing, $2N_f$ is the number of half cycles to failure and α is fatigue constant. As discussed before, the low-cycle fatigue parameters is related with buckling length, therefore the parameters of C_f and α are fitted for different slenderness ratios (L/D) respectively. As the derivation in Eq. (2), the $\ln(\varepsilon_p)$ and $\ln(2N_f)$ is negatively correlated. Assuming following the normal distribution, the fitted low-cycle fatigue parameters and correlation coefficient (R^2) are shown in Table 4. We can see from the Table 4 that all correlation coefficients R^2 are both bigger than 0.90 and thus the low-cycle fatigue equation adopted in this paper is reasonable.

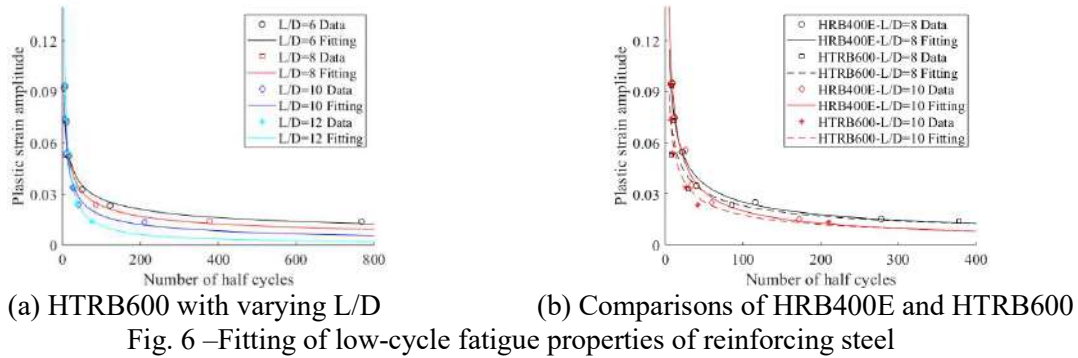
$$\varepsilon_p = C_f (2N_f)^{-\alpha} \quad (1)$$

$$\ln(\varepsilon_p) = \ln(C_f) - \alpha \ln(2N_f) \quad (2)$$

Table 4 – Low-cycle fatigue life fitting parameters of reinforcing steel material

Steel class		HRB400E			HTRB600		
Low-cycle fatigue parameters		C_f	α	R^2	C_f	α	R^2
L/D	6	0.15	0.38	0.99	0.26	0.47	0.99
	8	0.18	0.45	0.91	0.26	0.51	0.99
	10	0.21	0.54	0.95	0.40	0.65	0.97
	12	0.54	0.84	0.98	0.46	0.69	0.96

To further reveal the influence factors of low-cycle fatigue for reinforcing steel, the comparisons of low-cycle fitting curves are shown in Fig.6. We can see from Fig.6(a) that the the low-cycle fatigue life significantly decreases with the increase of slenderness ratio (L/D). Besides, the low-cycle fatigue life of HSSB HTRB600 is smaller than CBS HRB400E when total plastic strain is bigger than 0.02, as shown in Fig.6(b). This is worth noting because the longitudinal bars in RC columns are vulnerable to suffer larger cyclic strain amplitude at strong earthquake loading.



3.2 RC piers

The RC piers tested in this paper showed typical flexural failure modes and following failure phenomenon occurred in turn: cracking of cover concrete, yield of longitudinal bars, spalling and significant spalling of cover concrete, finally buckling and low-cycle fatigue fracture of longitudinal bars, as shown in Fig.7. The representative hysteretic curves of RC piers are shown in Fig.8.

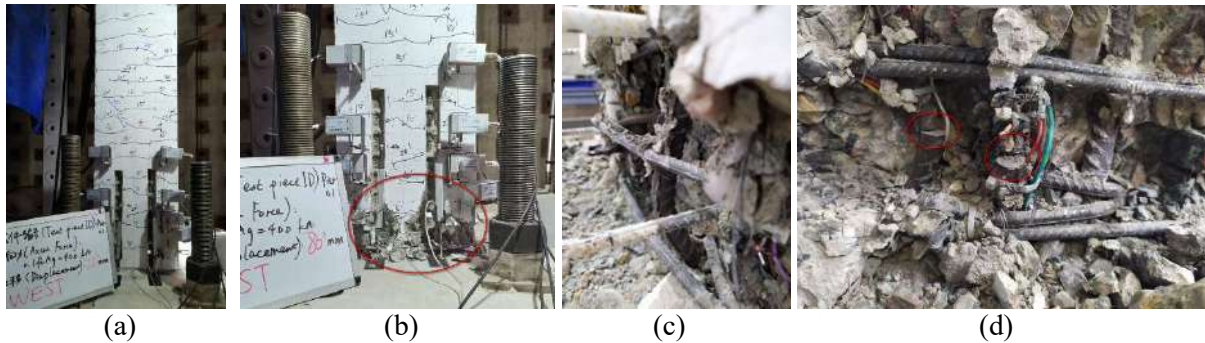


Fig. 7 –The damage development progress of RC piers: (a) cracking (b) spalling of cover concrete (c) buckling of longitudinal bar (d) low-cycle fatigue fracture of longitudinal bar

In order to further compare the effects of different parameters on seismic performance of RC piers, the key seismic performance indexes including yield displacement (Δ_y), yield drift ratio (δ_y), maximum bearing capacity (F_{max}), ultimate displacement (Δ_u), ultimate drift ratio (δ_u), displacement ductility (μ_Δ), plastic drift ratio (δ_p) as well as total hysteretic dissipated energy until specimen failure are calculated and shown in Table 5. Wherein, the idealized yield displacements are calculated according to the method proposed by R.Park[29] and the theoretical failure point is defined as the point when the remaining bearing capacity at post-peak stage dropped to 80% of the maximum lateral load. In addition, the skeleton curves and hysteretic dissipated energy curves are used to compare the seismic performance of RC piers.

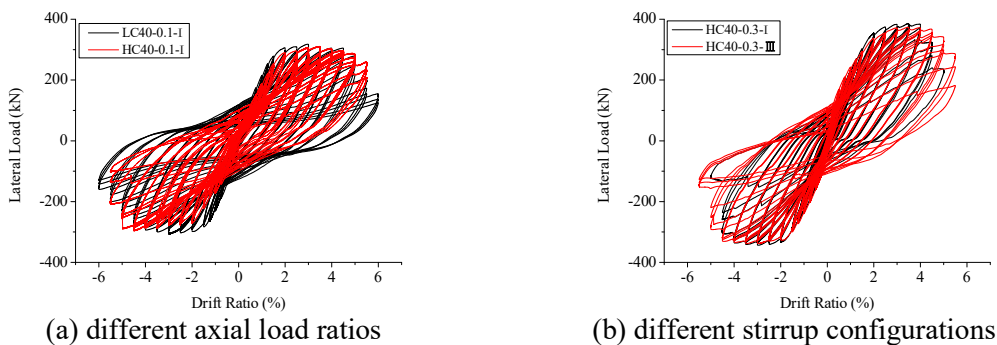


Fig. 8 –Hysteretic curves of RC piers

Table 5 – Summary of lateral bearing capacity, deformation, ductility and total hysteretic energy



Specimen	Δ_{yI} (mm)	F_{max} (kN)	Δ_u (mm)	δ_y (%)	δ_u (%)	μ_Δ	δ_p (%)	E_{hyst} (kJ)
LC40-0.1-I	25.00	303	100	1.25	4.99	4.00	3.74	474
HC40-0.1-I	27.96	304	103	1.40	5.13	3.67	3.73	368
H(V)C40-0.1-I	31.64	407	111	1.58	5.54	3.50	3.96	530
HC40-0.1-I-C	25.56	310	96	1.28	4.79	3.75	3.51	320
HC60-0.1-I-C	24.57	318	102	1.23	5.09	4.14	3.86	443
HC80-0.1-I	20.61	310	86	1.03	4.31	4.18	3.28	315
HC40-0.3-I	24.05	360	92	1.20	4.59	3.82	3.39	321
HC40-0.1-II	24.62	304	103	1.23	5.15	4.19	3.92	447
HC40-0.1-III	27.98	315	108	1.40	5.42	3.87	4.02	452
HC40-0.3-III	23.56	354	105	1.18	5.23	4.44	4.05	471

First of all, considering the cover concrete outside the longitudinal bar in plastic hinge region for most of the RC piers tested in this paper are removed for better observing the bar buckling, the effect of cover concrete is studied. As comparisons in Table 5 and Fig.9, the partly removing of cover concrete will slightly reduce the initial stiffness of RC piers and thus increase the yield displacement of RC piers. However, the partly removing of cover concrete doesn't obviously affect the ultimate deformation capacity of RC piers. As a result, the RC piers conducted in this paper can be used to compare the effects of different factors on the seismic performance of RC piers.

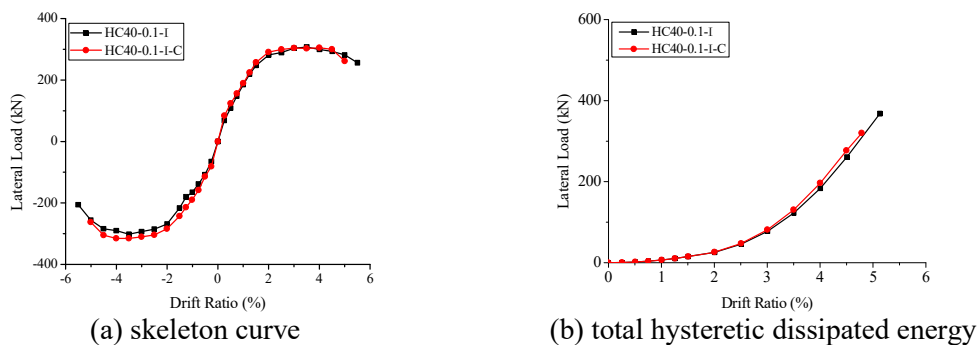


Fig. 9 –The effects of cover concrete on seismic performance of RC piers:

The effects of yield strengths of longitudinal bars on seismic performance of RC piers are studied by comparing the specimens of LC40-0.1-I, HC40-0.1-I and H(V)C40-0.1-I. Wherein the CSB HRB400E is used in specimen LC40-0.1-I, while the HSSB HTRB600 is adopted to replace HRB400E using equal strength and equal volume replacements for specimens HC40-0.1-I and H(V)C40-0.1-I respectively. We can see from Fig.10 and Table 5 that using HSSB with equal volume replacement obviously enhance the maximum bearing capacity, total deformation capacity and total hysteretic dissipated energy of RC piers. The RC piers reinforced with HSSB show comparable total deformability when replacing CBS using equal strength replacement. However, the using of HSSB will enhance the yield displacement and thus reduce the displacement ductility as well as total hysteretic dissipated energy at same drift ratio.

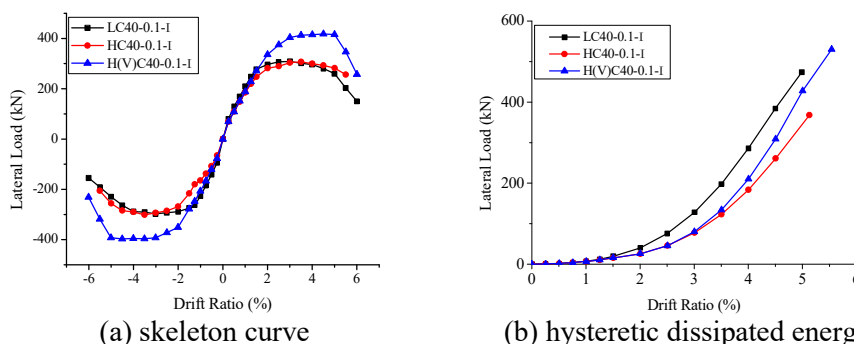
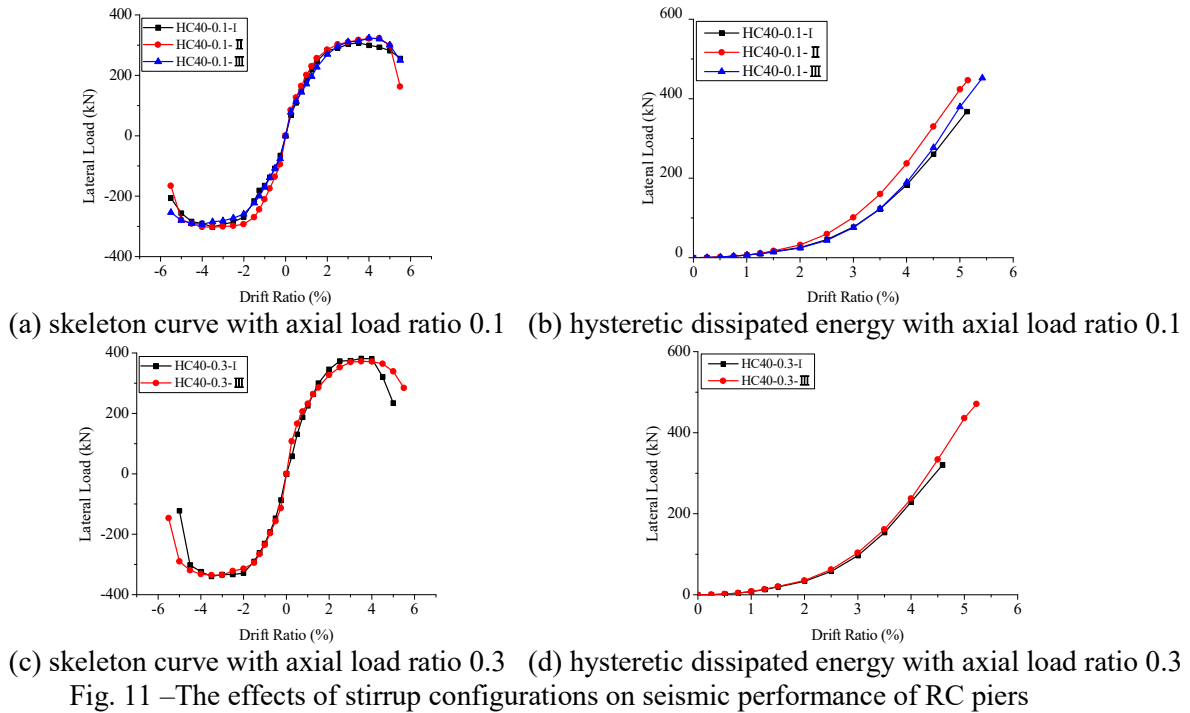


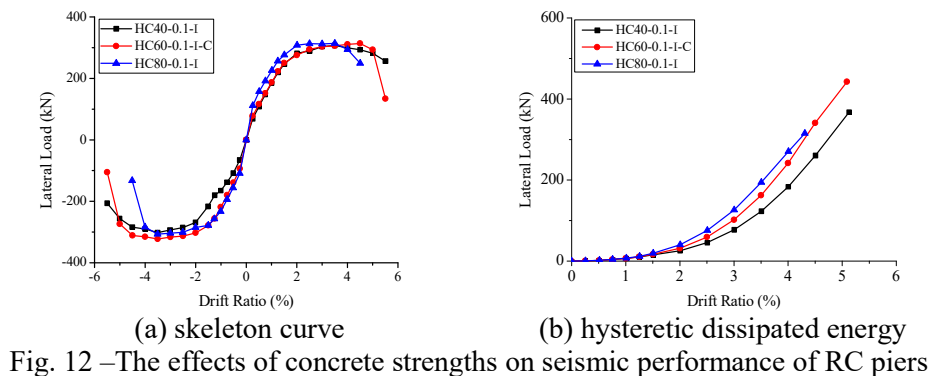
Fig. 10 –The effects of yield strengths of longitudinal bars on seismic performance of RC piers



The effects of stirrup configurations on seismic performance of RC piers are studied by comparing the specimens with different stirrup configurations and axial load ratios. The comparisons of specimens HC40-0.1-I, HC40-0.1-II and HC40-0.1-III indicate that the RC piers with type III stirrup show higher deformation capacity than that with type I and type II stirrups. It is because the type III stirrup could provide better constraint to resist the buckling of longitudinal bar. The conclusion is suitable for RC piers with high axial load (0.3), and the effects of stirrup configuration on deformation capacity is more pronounced for RC piers with high axial load.



The effects of concrete strengths on seismic performance of RC piers are studied by comparing the specimens HC40-0.1-I, HC60-0.1-I-C and HC80-0.1-I. We can see from Fig.12 and Table 5 that the increase in concrete strength will increase the initial stiffness and thus reduce the yield displacement of RC piers. Meanwhile, the using of higher strength concrete will reduce the deformation capacity and enhance the hysteretic dissipated energy at same drift ratio. It is worth noting that the influence extent intensifies with the increase of concrete strengths (i.e. the distinctions between C80 and C60 are bigger than C60 and C40).



The effects of axial load ratios on seismic performance of RC piers with different stirrup configurations are studied. We can see from Fig.13 and Table 5 that the increase of axial load ratio enhances the maximum bearing capacity and initial stiffness of RC piers. Meanwhile, the RC piers with high axial load ratio show worse deformation capacity. However, the decrease of deformation capacity for RC piers with the type III



stirrup is smaller than that with type I stirrup. It is because type III stirrup provide better constraints to prevent buckling of longitudinal bars than type I stirrup.

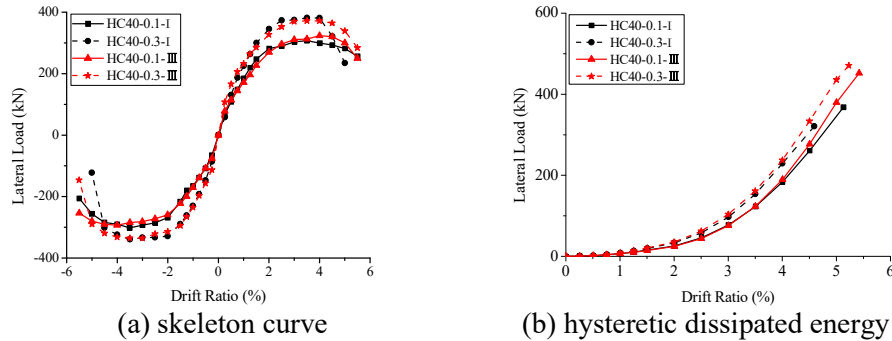


Fig. 13 –The effects of axial load ratios on seismic performance of RC piers

4. Numerical simulation

The Open System for Earthquake Engineering Simulation (OpenSees) program [30] is used to simulate the nonlinear response of RC piers. The fiber-based FEM in Ref. [31] is adopted in this paper and the detailed material selection and element division are shown in Fig.14.

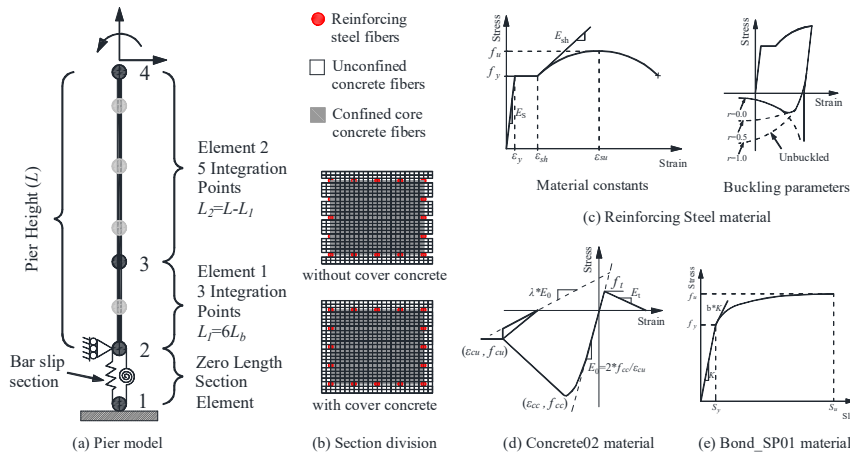


Fig. 14 –Fiber-based beam-column element model

In order to better consider the strength degradation of RC bridges under earthquake loading, the buckling and low-cycle fatigue of *reinforcing steel* material are taken into account. In addition, the effects of buckling on low-cycle fatigue of reinforcing steel is also considered. The low-cycle fatigue parameters (i.e. C_f and α) are selected according to Table 4 and the buckling length of longitudinal bar in RC piers. Wherein, the buckling length is calculated according to the buckling length calculation method recommended in Ref. [32].

To evaluate the numerical simulation method in this paper, the hysteretic curves and total hysteretic dissipated curves between experimental and numerical simulation are compared. We can see from Fig.15 and Fig.16 that the FEM used in this paper can simulate the hysteretic behavior, maximum bearing capacity, deformation capacity and hysteretic dissipated energy of RC piers with different yield strengths of longitudinal bars, concrete strengths, axial load ratios as well as stirrup configurations. In addition, the FEM could predict the strength degradation of RC piers caused by low-cycle fatigue of reinforcing steel. The type III stirrup provide better constraints to prevent buckling of longitudinal bars than that of type I and II configurations, thus the RC piers with type III stirrup configuration has smaller bar buckling length and show better deformation capacity.

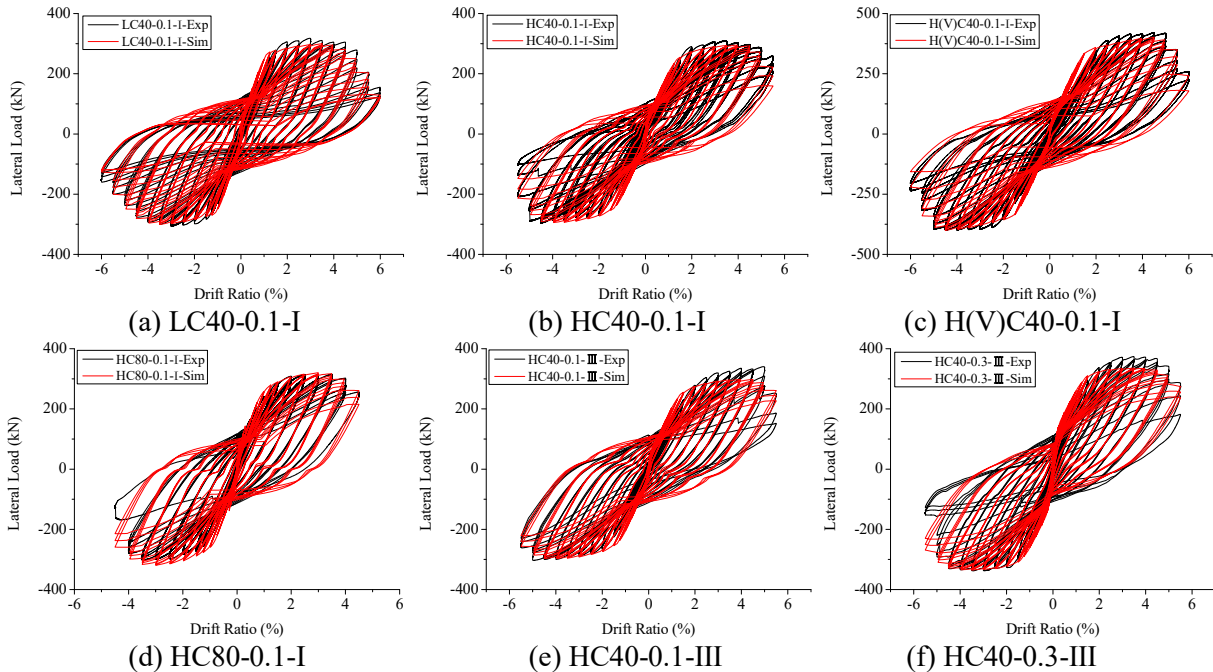


Fig. 15 –Comparisons of hysteresis curves between experimental and numerical simulation results

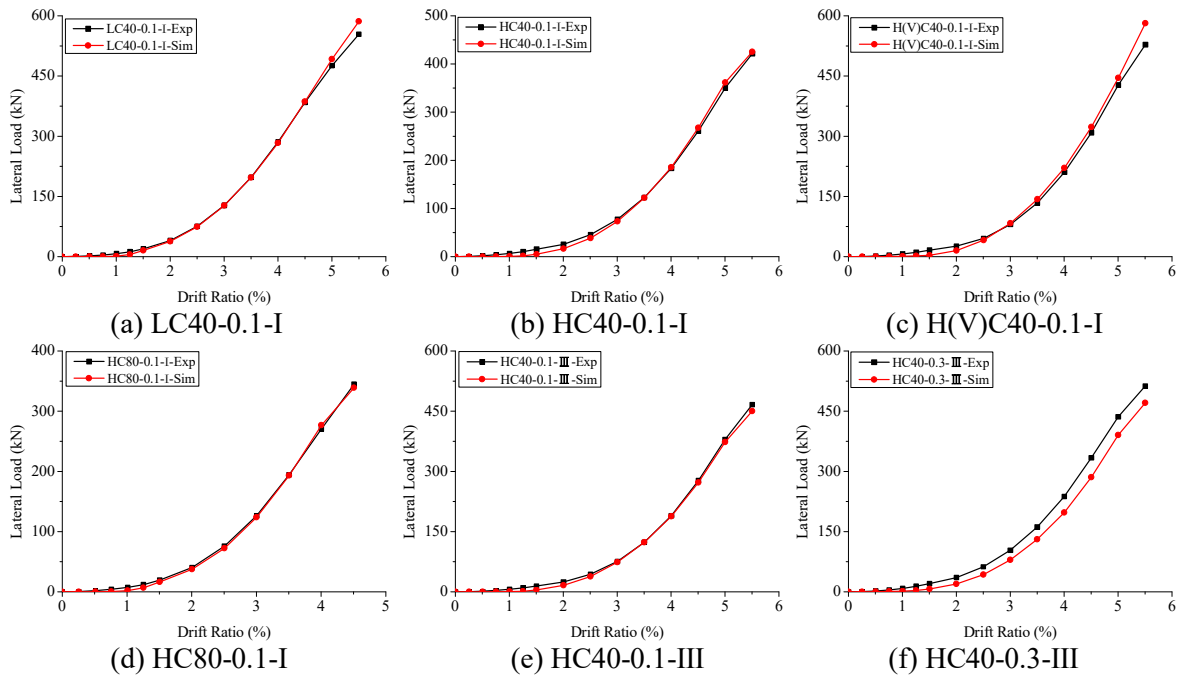


Fig. 16 –Comparisons of hysteretic dissipated energy between experimental and numerical simulation results

5. Conclusion

The tensile, compression and low-cycle fatigue properties of CSB (HRB400E) and HSSB (HTRB6000) were conducted. On this basis, the seismic performance of RC piers with different yield strengths of steel bars, concrete strengths, axial load ratios and stirrup configurations were studied. In addition, the numerical simulation of RC piers were conducted based on fiber-based FEM considering buckling and low-cycle fatigue of steel bars as well as bond slip (strain penetration) between longitudinal bar and concrete. Combined with the experimental investigations and numerical simulation, the following conclusions can be made.



(1) The HSSB (HTRB600) shows good tensile ductility (i.e., the fracture elongation and the ultimate uniform elongation). The compressive strain softening intensifies with the increase of slenderness ratio (L/D) and yield strengths of reinforcing steel. In addition, the low-cycle fatigue life obviously reduces with the increase slenderness (L/D).

(2) When HSSB (HTRB600) are used to replace CBS (HRB400E) with equivalent volume (one-to-one) replacement, the lateral bearing capacity and hysteretic dissipated energy increase as expected. While the RC piers show comparable lateral bearing capacity and deformation capacity when using HSSB to replace CBS with equal strength replacement.

(3) The increase in concrete compressive strength reduces the yield displacement of RC piers, thus leads to the increase of plastic deformation at same total deformation. As a result, the RC piers reinforced with higher strength concrete show bigger hysteretic energy dissipation capacity at same total drift ratio. However, the adoption of high strength concrete will reduce the deformation capacity of RC piers, and the influence extent intensifies with the increase of concrete strength.

(4) The RC piers with type III stirrup show higher deformation capacity than that with type I and type II stirrups. It is because the type III stirrup provide better constraint to resist the buckling of longitudinal bar. The effects of stirrup configuration on deformation capacity of RC piers is more pronounced under high axial load ratio, it is because longitudinal bar is more prone to buckling failure under high axial load ratio.

(5) The yield displacement reduces and the lateral bearing load increases with the increase of axial load ratio of RC piers. Meanwhile, the deformation capacity reduces for RC piers with high axial load ratio. However, the decrease degree of deformation capacity for RC pier with type III stirrup is relatively smaller than type I and type II stirrups.

6. References

- [1] Su, J., Wang, J., Li, Z., & Liang, X. (2019): Effect of reinforcement grade and concrete strength on seismic performance of reinforced concrete bridge piers. *Engineering Structures*, 198, 109512.
- [2] Rautenberg, J. M., Pujol, S., Tavallali, H., & Lepage, A. (2012): Reconsidering the use of high-strength reinforcement in concrete columns. *Engineering Structures*, 37, 135-142.
- [3] Rautenberg, J. M., Pujol, S., Tavallali, H., & Lepage, A. (2013): Drift capacity of concrete columns reinforced with high-strength steel. *ACI Structural Journal*, 110(2), 307-317.
- [4] Cheng, M. Y., & Giduquio, M. B. (2014): Cyclic Behavior of Reinforced Concrete Flexural Members Using High-Strength Flexural Reinforcement. *ACI Structural Journal*, 111(4), 893-902.
- [5] Tavallali, H., Lepage, A., Rautenberg, J. M., & Pujol, S. (2014): Concrete Beams Reinforced with High-Strength Steel Subjected to Displacement Reversals. *ACI Structural Journal*, 111(5), 1037-1047.
- [6] Barbosa, A. R., Link, T., & Trejo, D. (2016): Seismic performance of high-strength steel RC bridge columns. *Journal of Bridge Engineering*, 21(2), 04015044.
- [7] Trejo, D., Link, T. B., & Barbosa, A. R. (2016): Effect of Reinforcement Grade and Ratio on Seismic Performance of Reinforced Concrete Columns. *ACI structural journal*, 113(5), 907-916.
- [8] Palermo A, Liu R, Rais A, McHaffie B, Andisheh K, Pampanin S, Gentile R, Nuzzo I, Granerio M, Loporcaro G, McGann C & Wotherspoon L. M. (2017): Performance of road bridges during the 14 November 2016 Kaikoura Earthquake. *Bulletin of the New Zealand Society for Earthquake Engineering*, 50(2),253-270.
- [9] Gomes, A., & Appleton, J. (1997): Nonlinear cyclic stress-strain relationship of reinforcing bars including buckling. *Engineering Structures*, 19(10), 822-826.
- [10] Dhakal, R. P., & Maekawa, K. (2002): Path-dependent cyclic stress-strain relationship of reinforcing bar including buckling. *Engineering Structures*, 24(11), 1383-1396.
- [11] Kunnath, S. K., Heo, Y., & Mohle, J. F. (2009): Nonlinear uniaxial material model for reinforcing steel bars. *Journal of Structural Engineering*, 135(4), 335-343.



- [12] Lopes, A. V., Lopes, S. M., & do Carmo, R. N. (2012): Effects of the compressive reinforcement buckling on the ductility of RC beams in bending. *Engineering Structures*, 37, 14-23.
- [13] Dhakal, R. P., & Su, J. (2018): Design of transverse reinforcement to avoid premature buckling of main bars. *Earthquake Engineering & Structural Dynamics*, 47(1), 147-168.
- [14] Girgin, S. C., Moharrami, M., & Koutromanos, I. (2018): Nonlinear beam-based modeling of RC columns including the effect of reinforcing-bar buckling and rupture. *Earthquake Spectra*, 34(3), 1289-1309.
- [15] Gkimousis, I., & Koumousis, V. (2018): Modeling RC column flexural failure modes under intensive seismic loading. *Earthquake Engineering & Structural Dynamics*, 47(9), 1942-1962.
- [16] Dhakal, R. P., & Maekawa, K. (2002): Modeling for postyield buckling of reinforcement. *Journal of structural engineering*, 128(9), 1139-1147.
- [17] Ghannoum, W. M., & Slavin, C. M. (2016): Low-cycle fatigue performance of high-strength steel reinforcing bars. *ACI Materials Journal*, 113(6), 803.
- [18] Kashani, M. M., Barmi, A. K., & Malinova, V. S. (2015): Influence of inelastic buckling on low-cycle fatigue degradation of reinforcing bars. *Construction and Building Materials*, 94, 644-655.
- [19] Tripathi, M., Dhakal, R. P., Dashti, F., & Massone, L. M. (2018): Low-cycle fatigue behaviour of reinforcing bars including the effect of inelastic buckling. *Construction and Building Materials*, 190, 1226-1235.
- [20] GB1499.2-2018 (2018): Steel for the reinforcement of concrete-Part 2: Hot rolled ribbed bars. Beijing, China: Standard Press of China. (in Chinese)
- [21] GB50010 (2015): Code for design of concrete structures. Beijing, China: Ministry of Housing and Urban-rural Development. (in Chinese)
- [22] JTG 3362-2018 (2018): Specifications for Design of Highway Reinforced Concrete and Prestressed Concrete Bridges and Culverts. Beijing, China: Ministry of Transport of the People's Republic of China. (in Chinese)
- [23] Fu, J., Wu, Y., & Yang, Y. B. (2015): Effect of reinforcement strength on seismic behavior of concrete moment frames. *Earthquake and Structures*, 9(4), 699-718.
- [24] Li, Y., Cao, S., & Jing, D. (2018): Concrete Columns Reinforced with High-Strength Steel Subjected to Reversed Cycle Loading. *ACI Structural Journal*, 115(4), 1037-1048.
- [25] GB/T228.1 (2010): Metallic Materials-tensile Testing-Part 1: Method of Test at Room Temperature. Beijing, China: Standardization Administration of the People's Republic of China & General Administration of Quality Supervision, Inspection and Quarantine of the People's Republic of China. (in Chinese)
- [26] GB/T50152 (2012): Standard for Test Method of Concrete Structures. Beijing, China: China Architecture & Building Press. (in Chinese)
- [27] Coffin Jr, L. F. (1954). A study of the effects of cyclic thermal stresses on a ductile metal. *Transactions of the American Society of Mechanical Engineers*, New York, 76, 931-950.
- [28] Manson, S. S. (1953). Behavior of materials under conditions of thermal stress (Vol. 2933). National Advisory Committee for Aeronautics.
- [29] Park, R. (1989). Evaluation of ductility of structures and structural assemblages from laboratory testing. *Bulletin of the New Zealand Society for Earthquake Engineering*, 22(3), 155-166.
- [30] McKenna, F., Fenves, G. L., & Scott, M. H. (2010). Open system for earthquake engineering simulation. University of California, Berkeley, CA.
- [31] Su, J., Li, Z., Wang, J., & Dhakal, R. P. (2020). Numerical simulation and damage analysis of RC bridge piers reinforced with varying yield strength steel reinforcement. *Soil Dynamics and Earthquake Engineering*, 130, 106007.
- [32] Su, J., Wang, J., Bai, Z., Wang, W., & Zhao, D. (2015). Influence of reinforcement buckling on the seismic performance of reinforced concrete columns. *Engineering Structures*, 103, 174-188.